Estimating long-term soil respiration rates from carbon isotopes occluded in gibbsite

Paul A. Schroeder *, Jason C. Austin, John F. Dowd

Department of Geology, 210 Field St., University of Georgia, Athens, GA 30602-2501, USA

Abstract

Carbon occluded in the soil gibbsite crystal structure at the Panola Mountain Research Watershed, Georgia, U.S. is presumed to be in isotopic equilibrium with the CO_2 respired from soil organics by microbes and plant roots. Fitting of the stable carbon isotopic data to a Fickian diffusion-based depth function results in an estimate of 47 gC m^{-2} y^{-1} for the long-term soil respiration rate. A numerical model that includes depth-dependent production and diffusion terms results in estimates of 28–12 gC m^{-2} y^{-1}. These values range from 15 to 50 times less than the average of modern values for mixed deciduous forests in wet temperate climates. This disparity has several implications for our understanding of the geologic record of climate change, which include: (1) evidence for a cooler and seasonally drier climate during the mid-Holocene in the southeastern U.S., or (2) fluxes of carbon from the soil pool as recorded by soil mineral proxies (i.e., long-term soil respiration rates) under estimate atmosphere annual carbon flux measurements (i.e., short-term measures), and (3) the need to refine soil respiration models used to relate palesol stable carbon isotopic measurements to paleo-atmospheric P_{CO_2} estimates.
© 2006 Elsevier Inc. All rights reserved.

1. Introduction

It is estimated that today's net flux of carbon from the Earth's terrestrial soil and detritus reservoir to its atmospheric reservoir is approximately 76 Pg C y^{-1} (Raich and Potter, 1995). The atmospheric carbon pool is estimated to be nearly 720 Pg, which is about half that of the reduced carbon in the soil and detritus pool (Berner and Berner, 1987). Hence, it can be approximated that about 10% of the atmosphere's carbon passes through the Earth's land surface each year through the process of "soil respiration." The total CO_2-production by microbial and root metabolic processes is herein defined as soil respiration. The role of soil respiration and its sensitivity to elevated temperatures serves to be a potentially important feedback mechanism in the regulation of the earth's carbon cycle (Boone et al., 1998), particularly as carbonic acid is generated for

reaction with rocks and the subsequent return of bicarbonate to the oceans.

Real time CO_2 efflux measurements were first made using static 24 h alkali traps. More recently dynamic (infrared gas analyzer) chambers placed above the ground have provided abundant and accurate annual efflux data (Jensen et al., 1996). The following discussion assumes annual CO_2 efflux rate measurements are equivalent to modern soil respiration rates. Although today's estimates of soil respiration rates seem well constrained, our understanding of how soil respiration rates change over long periods of time (1000s of years) is poorly constrained. This is because there has not been a way to estimate these rates in residual weathering profiles with long exposure ages. Yapp and Poths (1994) estimate ancient soil CO_2 respiration rates from an Ordovician Neda Formation paleosol as being similar to modern soils using assumed soil properties and measure $\delta^{13}C$ values in carbon occluded in goethite. The purpose of this paper is to introduce the concept of a long-term soil respiration rate. This is a rate that represents the integrated soil respiration, recorded by authigenic minerals that have formed over

* Corresponding author. Fax: +1 706 542 2425.
  E-mail address: schroe@uga.edu (P.A. Schroeder).

a long period of time. The basis for this approach uses: (1) models for the depth distribution of stable carbon isotopes of soil CO_2 (e.g., Cerling, 1984), (2) the stable carbon isotopic signatures preserved in authigenic gibbsite, and (3) age constraints provided by cosmogenic dating of quartz near the soil surface ([10]Be and [26]Al) and gibbsite-bound CO_2(^{14}C).

2. Soil CO_2 models

Paleo-P_{CO_2} studies that utilized $\delta^{13}C$ in minerals are based on the model of (Cerling, 1984), which describes the steady-state one-dimensional Fickian diffusion of soil gases. This model is used to relate the $\delta^{13}C$ of soil minerals to the soil respiration rate (Q, units = gC m^{-2} h^{-1}). The analytical solution for the differential equation

$$\frac{dC_s^*}{dt} = 0 = D_s^* \frac{\partial^2 C_s^*}{\partial z^2} + \phi^* \tag{1}$$

with boundary conditions

$$z = L; \quad \frac{\partial C_s^*}{\partial z} = 0, \tag{2}$$

$$z = 0; \quad C_s^* = C_a^* \tag{3}$$

is

$$C_s^* = \frac{\phi^*}{D_s^*}\left(Lz - \frac{z^2}{2}\right) + C_a^*, \tag{4}$$

where D is the diffusion coefficient, with the superscript (*) representing bulk properties, and subscripts (s) and (a) representing soil CO_2 and atmosphere CO_2, respectively. The production rate of CO_2 in the soil is ϕ (i.e., $\phi = Q/L$) in units of gC cm^{-3} h^{-1}, where L is the characteristic depth (cm) below which C_s^* does not change. Below L (i.e., $z > L$) Eq. (4) is no longer applicable and does not consider CO_2 production, which reflects either the bottom of the soil profile or a point in the profile where production is so small it can effectively be considered zero.

The above analytical model requires that D_s^* is constant through the soil profile. Diffusion (D_s^*) is first approximated by using the diffusion coefficient of CO_2 in air (D_a^*) and, for the analytical solution, assuming typical soil gas-filled porosity (ε_g) and tortuosity (τ) factors.

$$D_s^* = D_a^* \varepsilon_g \tau. \tag{5}$$

If the diffusion terms vary as a function of depth (z), then the analytical solution Eq. (4) becomes invalid. Since ϕ and D_s^* do likely vary with depth in a weathering profile, we propose herein that a numerical finite difference model approach be employed to more accurately reconcile soil respiration rates as reflected in the isotopic signatures of minerals preserved in soil profiles. The function used to approximate the attenuation of ϕ with depth, is

$$\phi(z) = \phi_o^* e^{z/Z}, \tag{6}$$

where Z is the attenuation depth of the soil (Cerling, 1984). Fig. 1 shows the distribution of ϕ with depth using values of $Z = 10, 20, 50,$ and 100 cm. Stable carbon isotope compositions of the organic matter in temperate soil profiles (e.g., Schroeder and Melear, 1999) show isotopically heavier values in the top 20 cm, which supports the idea that carbon turnover is greatest in the upper A-horizon interval. This suggests that a Z value of 20 cm can realistically describes the production profile.

Water-filled pores reduce the effective porosity and modify gas diffusion. We assume that the difference between volumetric water content at 0 and -300 cm soil water pressure accurately reflects gas-filled porosity in a soil profile. The choice of -300 cm soil water pressure is based on the similarity of soil texture (i.e., % sand, silt, and clay) profiles studied by Bruce et al. (1983) and this study. The extensive data set of (Bruce et al., 1983) establishes the strong correlation between soil texture and the capillary soil water retention process in a Cecil soil in the southeastern U.S. A Cecil is a fine, kaolinitic, thermic Typic Kanhapludult (USDA-NRCS Soil Survey Division). We
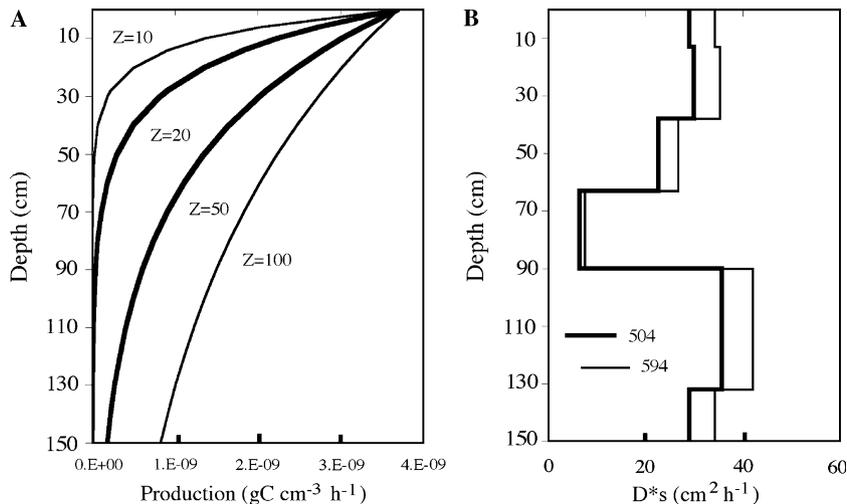

Fig. 1. Depth profiles of carbon production and soil diffusion coefficients used in numerical modeling scheme. (A) Production is simulated using Eq. (6), using Z values over the range of 10–100. (B) Diffusion is controlled by air-filled porosity and tortuousity. Values of 504 (bold) and 594 and a τ of 0.6 are assumed. The air-filled function is defined by the data set of Bruce et al. (1983). Using $D_{air}^* = 594$ resulted in lower soil respiration rates, therefore the smaller value of 504 was used in both analytical and numerical calculations.

therefore employ the physical characteristics of Cecil soils in the southeastern U.S. (Bruce et al., 1983) and assume that the measures of volumetric water content over the depth intervals of 10–16, 35–41, 60–66, 87–93, and 129–135 cm represent the distribution function for gas-filled porosity. For numerical modeling purposes, ε_g is defined by a step-wise function fitted to data of (Bruce et al., 1983). Fig. 1 shows step functions using a τ value of 0.6 and air diffusion coefficient values of 0.140 and 0.165 cm^2 s^{-1} (i.e., those cited by Cerling (1984) and Lasaga (1998)), respectively.

The final form of the finite difference model is given as

$$C_{si}^{*k+1} = \Delta t \left[D(z) \left(\frac{C_{i+1}^k - 2C_i^k + C_{i-1}^k}{\Delta z^2} \right) + \phi(z) \right] + C_i^k, \quad (7)$$

where Δt is the time step measured in seconds, $D(z)$ is the depth dependant function of D_s^*, $\phi(z)$ is the depth dependant function of ϕ^*, subscript i represents the depth, and superscript k represents the time step. The model is run until steady state is reached, solving for concentration of ^{12}C and ^{13}C, which are used to calculate the δ^{13}C of the soil CO$_2$.

The mass differences between ^{12}CO$_2$ and ^{13}CO$_2$ (mass 44 and 45, respectively) result in slight but important differences in their respective diffusion coefficients (D_s^{44} and D_s^{45}). Craig (1954) related the diffusion coefficients of the two isotopes by their atomic masses and the average mass of air (M^{44}, M^{45} and M_a, respectively) using the following equation

$$\frac{D_s^{44}}{D_s^{45}} = \left[\frac{(M^{44} + M_a)}{M^{44} M_a} \frac{M^{45} M_a}{(M^{45} + M_a)} \right]^{0.5}. \quad (8)$$

Likewise for the ratios of D_s^* to D_s^{44} and D_s^* to D_s^{45}, equations similar in form to Eq. (8) can be written. In the equations that follow the variables D^{12} and D^{13} will be used to denote the diffusion of the mass 44 and 45 (i.e., ^{12}CO$_2$ and ^{13}CO$_2$ molecules, respectively).

The concentration of ^{13}CO$_2$ in the profile is modeled by the following analytical solution

$$C_s^{13} = \frac{\phi^{13}}{D_s^{13}} \left(Lz - \frac{z^2}{2} \right) + C_a^{13}, \quad (9)$$

where C_a^{13}, C_s^{13} and ϕ^{13} are the ^{13}CO$_2$ concentrations in the atmosphere and soil and the ^{13}CO$_2$ production rate, respectively. The concentrations of ^{13}CO$_2$ are further defined by the isotopic ratio of ^{13}CO$_2$/^{12}CO$_2$ of the soil air (R_s), atmosphere (R_a) and respired CO$_2$, (R_ϕ). These relationships are:

$$C_s^{13} = C_s^* \left(\frac{R_s}{1 + R_s} \right), \quad (10)$$

$$C_a^{13} = C_a^* \left(\frac{R_a}{1 + R_a} \right), \quad (11)$$

and

$$\phi^{13} = \phi^* \left(\frac{R_\phi}{1 + R_\phi} \right). \quad (12)$$

Isotopic conventions report the isotopic ratio as a per mil value, using the notation:

$$\delta^{13}C_i = \left(\frac{R_i}{R_{PDB}} - 1 \right) 1000; \quad \text{for } \delta^{13}C_s, \delta^{13}C_a, \quad \text{and } \delta^{13}C_\phi, \quad (13)$$

where $\delta^{13}C_i$ is the value for soil air, atmosphere, and respired CO$_2$, respectively and R_{PDB} is the ratio for the Pee-dee Formation *Belemitella Americana* isotopic standard (Craig, 1957). By substitution of Eqs. (4), (7), and (8) into Eq. (13), (Cerling, 1984) developed an analytical model that describes the $\delta^{13}C_s$ composition of soil CO$_2$ as function of depth in the profile, the $\delta^{13}C_a$ composition of the atmosphere, soil CO$_2$ production rate and the $\delta^{13}C_\phi$ composition of the respired CO$_2$. The form of this equation is as follows:

$$\delta_s = \left(\frac{1}{R_{PDB}} \left[\frac{\left[\frac{\phi^*}{D_s^*} \left(Lz - \frac{z^2}{2} \right) \right] \left[\frac{D_s^*}{D_s^{13}} \right] [\bar{\delta}_\phi] + C_a^* \bar{\delta}_a}{\left[\frac{\phi^*}{D_s^*} \left(Lz - \frac{z^2}{2} \right) \right] \left[1 - \frac{D_s^*}{D_s^{13}} \bar{\delta}_\phi \right] + C_a^* [1 - \bar{\delta}_a]} \right] - 1 \right) 1000, \quad (14)$$

where

$$\bar{\delta}_i = \left[\frac{\left(\frac{\delta_i}{1000} + 1 \right) R_{PDB}}{1 + R_{PDB} \left(\frac{\delta_i}{1000} + 1 \right)} \right]. \quad (15)$$

Table 1
Constant/variable parameter coefficients and values used in modeling schemes

	Q	L	D_s^*	$\bar{\delta}_\phi$	C_a^*	$\bar{\delta}_a$	Z
Analytical solution							
Value	5.322×10^{-7}[a]	150	72.58	1.0817×10^{-2}	1.248×10^{-7}	1.1046×10^{-2}	∞
Units	gC cm^{-2} h^{-1}	cm	cm^2 h^{-1}	Ratio	gC cm^{-3}	Ratio	cm
Alternate values	47[a]	1.5	0.02016	-27[b]	250	-6[b]	∞
Units	gm^{-2} y^{-1}C	m	cm^2 s^{-1}	‰	ppm	‰	cm
Numerical solution							
Value	28	150	$72.58 \times f(z)$	1.0817×10^{-2}	1.248×10^{-7}	1.1046×10^{-2}	20
Value	12	150	$72.58 \times f(z)$	1.0817×10^{-2}	1.248×10^{-7}	1.1046×10^{-2}	50
Units	gC m^{-2} y^{-1}	cm	cm^2 h^{-1}	Ratio	gC cm^{-3}	Ratio	cm

[a] Best-fit solution.
[b] Per mil value used in Eq. (13) to derive $\bar{\delta}_\phi$ and $\bar{\delta}_a$ values.

Table 2
Stable carbon isotopes from gibbsite dehydroxylation and associated and cosmogenic carbon results from the <2 μm fraction of samples from the Panola Mountain ridge crest site

Sample ID Panola Pit #1	Depth (cm) (horizon)	$\delta^{13}C$ (‰)	Model ^{14}C age (years)[a]
PP1-3	6 (A)	−12.0	3700
PP1-5	14 (B)	−13.4	2700
PP1-6	28 (B)	−14.7	4200
PP1-7	51 (B)	−16.7	7900
PP1-13	160 (C)	−20.9	—
PP1-15	236 (C)	−19.5	8000

[a] Ages are radiocarbon years using the Libby half-life of 5568 years and following the conventions of Stuiver and Polach (1977).

The process of fitting the observed $\delta^{13}C$ values and depth values to the analytical function is accomplished by estimating values for the parameters in Eq. (14). The soil respiration parameter Q is left as an independent variable, and the data are fit via a least-squares minimization process. Table 1 itemizes variables used in both the analytical and numerical solutions. All minimization calculations were conducted using the computer program MacCurveFit (Raner, 1998). The process of best fitting the observed and calculated $\delta^{13}C$ values from the numerical function is accomplished by visual inspection of forward modeling results using Eq. (10) and varying the input parameters of Z and ϕ^*.

3. Study site and sampling methods

The investigation was conducted at the Panola Mountain Research Watershed (PMRW) operated by United States Geological Survey (USGS) located in the Georgia Piedmont of the southeastern United States (Huntington, 1995; Schroeder and Melear, 1999). Sampling occurred at a summit site in the PMRW where the weathering profile is believed to be wholly residual (i.e., not colluvial). Six samples were collected from a 1 m^2 pit at specified depths (see Table 2).

Details of the CO_2 extraction process are described by Schroeder and Melear (1999) and are briefly outlined here. Pretreatment included particle size separation (<2 μm), repeated H_2O_2 digestions and low temperature (200 °C) O_2 combustion to remove organic matter. CO_2 is released upon thermal breakdown at 230° to 240°C under vacuum in the laboratory. CO_2 produced from the breakdown of gibbsite was cryogenically trapped, and isotopic analyses were conducted at the University of Georgia Stable Isotope Facility. Additional details regarding sample properties can be found in the work by Schroeder et al. (2001) who examined the same samples for their cosmogenic ^{14}C, ^{10}Be and ^{26}Al properties.

4. Results

Table 2 contains a summary of sampling depths and average stable carbon isotopic values of the gibbsite-bound CO_2 (see Table 2 from Schroeder et al., 2001, and Table 1 from Schroeder and Melear, 1999). Fig. 2 is a depth plot of the isotopic data with ±1.5‰ error bars. This error represents the maximum isotopic range observed during replicate analyses. Also found in Table 2 are the average model ^{14}C ages of the gibbsite-bound CO_2. As discussed by Schroeder et al. (2001), the model ^{14}C age of the gibbsite deep in the weathering profile (C-horizon) at PMRW suggests an average age of mineralization of about 8000 years. Samples from the A- and B-horizons reveal much younger gibbsite ages of 2700–4200 years. The age differences of secondary minerals in the upper and lower horizons indicate that significant crystallization occurs as the weathering front propagates downward into the landscape. Inventories of *in situ* cosmogenic ^{10}Be and ^{26}Al abundances in surface samples indicate a minimum residence time of 90 kyr (Schroeder et al., 2001). The disparity of ^{14}C gibbsite ages and *in situ* cosmogenic residence times points to the geologically young age of secondary mineralization as well as the multi-generational nature of regolith components (Melear, 1998).

4.1. Analytical solution

A least-squares minimization approach was initiated with the parameter values suggested by Schroeder and Melear (1999). In all cases, the sum of the squares error (sse) was evaluated to assess the goodness of fit [sse equals $\sum (y_i − f(x_i))^2$ where y_i and x_i are the data pairs and the correlation coefficient r^2 equals $(n * \text{sse})/n \sum y_i^2 − (\sum y_i)^2$ where n is the number of data points]. L, D_s^*, and R_{PDB} were held constant with the values of 150 cm, 72.6 cm^2 h^{-1}, and 0.0112372, respectively. The characteristic depth of

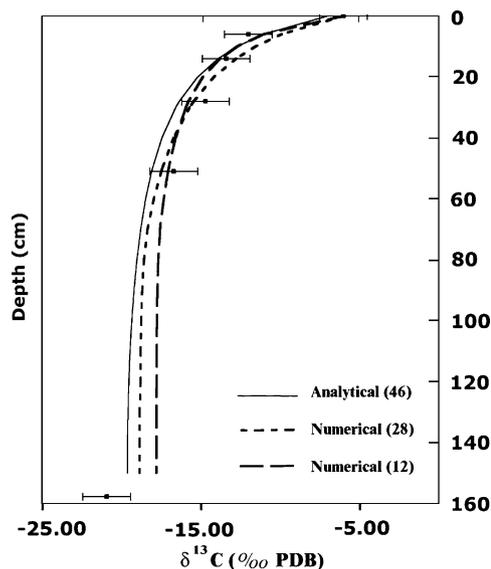Fig. 2. Depth profile plot of $\delta^{13}C$ values from gibbsite-bound CO_2 in the ridge crest site at the PMRW (black squares). Error bars reflect maximum range in values observed in replicate analyses. The solid line represents the least-squares fit to the analytical model solution Eq. (10). The thin lines represent numerical solutions using D_{air}^*, and Z, values of 504 cm^2 h^{-1} and 20 cm (long dashed line), and 50 cm (short dashed line). Parenthetic values are soil respiration rates in g m^{-2} y^{-1}. Sample from 236 cm not plotted.

150 cm was based on estimates for average Georgia Piedmont A–B horizon thickness (Schroeder and West, 2005). The choice of the D^* value was based on the CO_2 in air, typical soil porosity, and tortuosity (Cerling, 1984). Starting values for the atmospheric concentration of CO_2, δ_s, and δ_a were 250 ppm, $-27\permil$, and $-6\permil$, respectively. These starting values were based on an average of post- and pre-industrial atmospheric concentration and isotopic composition and measured isotopic composition of the input soil organic matter (Schroeder and Melear, 1999).

During the first pass at minimization of Eq. (14), only Q was allowed to vary. This resulted in a fit where $Q = 5.32 \times 10^{-7}$ gC cm^{-2} h^{-1} (46.6 gC m^{-2} y^{-1}) with sse = 7.79 ($r^2 = 0.937$). Further model optimizations were attempted by allowing the isotopic composition of the atmosphere, the soil organic matter input and the atmospheric concentration of CO_2 to be variable coefficients. Negligible improvement in the sse occurred as each $\bar{\delta}_\phi$, $\bar{\delta}_a$, and C_0^* coefficient was used in the optimization. Table 1 contains the best-fit value for Q, and Fig. 2 graphically shows the solution for the function.

4.2. Numerical solution

The series of numerical solutions shown in Fig. 2 where chosen on the basis of a visual best-fit while maintaining physically realistic coefficients in the solution. A D_a^* value of 0.140 cm^2 s^{-1} was used with its value modified by the distribution function shown in Fig. 1. Solutions for $Z = 20$ and 50 cm are shown in Fig. 2. The effect of increasing the interval of production to $Z = 50$ cm resulted in a fit visually closer to the observed data when compared to a smaller production interval of $Z = 20$ cm. In order to maintain a fit with the observed data, soil respiration rates needed to be set to values of 28 and 12 gC m^{-2} y^{-1} for models runs using Z values of 20 and 50 cm for production, respectively. Model runs using soil respiration rates of >28 gC m^{-2} y^{-1} required physically unreasonable assumptions for diffusion and production distribution functions.

The data points beyond the characteristic depth (150 cm) used in this study do not fit the model profiles. The model ^{14}C ages for these samples in the deep C-horizon are notably older than the samples in the A–B-horizons (~8000 years versus 2700–4200 years). These differences support the notion that the some of the gibbsite population exhibits more than one crystallization event. Since there are no gibbsite age studies of weathering profiles from the surface to bedrock at this locality, the testable hypothesis is that gibbsite ages should become youngest at the incipient saprolite–bedrock interface.

5. Discussion

Analytical and numerical estimates for the long-term soil respiration rates using gibbsite-bound δ^{13}C in the temperate deciduous forest at PMRW result in a range from 28 to 12 gC m^{-2} y^{-1}. These rates are 15–50 times less than the modern global estimates of 647 gC m^{-2} y^{-1} for similarly vegetated terrain (Raich and Schlesinger, 1992). This suggests that the time-integrated soil respiration rates, proxied by the carbon isotopic signature in authigenic gibbsite, reflect a period of significantly lower CO_2 flux to the atmosphere. On a global scale, soil respiration rates show a generally positive correlation with mean annual air temperature (T) and precipitation (P). The various correlations between global soil respiration rates and T or P proposed by Raich and Schlesinger (1992), although all positive, are too poor to allow for a precise estimate of T or P. The positive correlations do suggest, however, that the main factor that can account for the low soil respiration rate in our study is the influence of a cooler and perhaps a more monsoonal type climate during the time period represented by the model ^{14}C ages. Radiocarbon dates of large paleomeanders in the southeast Georgia (Leigh and Feeney, 1995) indicate monsoonal conditions may have been regionally active 8500–4500 years ago.

Pollen studies by Brook (1996) conclude that the southeastern U.S. has undergone a general transition from deciduous hardwood forests (10,000–5000 years ago) to pine dominated forests (5000–0 years ago). However, as noted by Jackson and Whitehead (1993), the chronological reliability of wetland cores are often compromised by hiatuses, irregular sedimentation rates and erroneous ^{14}C dates for sediments. The soil respiration rates found in this study are similar to the modern annual CO_2 flux measured on tundra and desert scrub terrain (Raich and Schlesinger, 1992). There is no suggestion that PMRW on the Piedmont of the southeastern United State was occupied by such vegetation; however, it appears that it was a terrain whose respiration rates were limited by temperatures and annual precipitation amounts that are lower than those of today. It is proposed that the climatic record being preserved by the gibbsite in the residual weathering profile reflects a long integrated period where perhaps the southeastern U.S. climate was cooler and precipitation was seasonal. As noted by Brook et al. (1983), rates of soil respiration are better linked to actual evapotranspiration rates (actual H_2O loss to the atmosphere). The estimated low respiration rates then indicate that in the southeastern U.S. during the Holocene the evapotranspiration rates were also lower than today.

Another implication for the low long-term soil respiration rate estimate is the need to more closely evaluate the implicit assumptions in the soil respiration model. The assumption about negligible isotopic fractionation between the respired soil CO_2 and the carbon occluded into gibbsite requires more investigation. The assumption about a steady-state dynamic equilibrium between the rate of weathering and the rate of mass loss due to chemical and physical erosion needs testing, for example, by employing cosmogenic nuclides ^{10}Be and ^{26}Al throughout the entire weathering profile.

A final implication of the low respiration rate estimate concerns the broader issue of long-term versus short-term rate measurements. If the lower rates recorded by the

minerals are not reflecting cooler and/or dryer climates, there needs to be a reconciliation of long-versus short-term rate measurements. This is a common problem in the geologic record, where geologic processes operate in time scales from seconds to millions of years. It is recognized in many geologic instances that long-term rate estimates are orders of magnitude lower than the short-term estimates. Examples include long-versus short-term rates of silicate weathering (White, 1995) and rates of sedimentation (Anders et al., 1987), where instantaneous rates overestimate the continuity of processes that operate over long periods of time (i.e., episodic rates). The preliminary results from this study suggest that if paleo-P_{CO_2} equations use soil mineral $\delta^{13}C$ gradients to calculated paleo-P_{CO_2} concentrations, then the assumed respiration rates used might require adjustments to reflect the differences.

Future research will need to discern whether this low respiration rate estimate is a consequence of (1) a period of climate conditions in the southeastern U.S., where temperatures were lower and precipitation events were more seasonal than the modern climate, (2) an artifact of comparing short-term versus long-term rate measurements, or (3) inadequacies in the model assumptions.

6. Conclusions

Numerical modeling of $\delta^{13}C$ values from gibbsite at the Panola Mountain Research Watershed results in soil respiration rate estimates 15–50 times lower than modern annual carbon flux measurements from the same environments. Additional field measurements and model refinements are needed to better constrain this estimate of average soil respiration rates for the Holocene. These results are consistent with our current understanding that during the mid-Holocene the southeastern United States was slightly cooler and seasonally drier than today. Alternatively, long-term respiration rates may be lower because modern measured carbon efflux is biased to indicate higher short-term rates.

Acknowledgments

Associate editor: Tim Lyons

References

Anders, M.H., Krueger, S.W., Sadler, P.M., 1987. A new look at sedimentation rates and the completeness of the stratigraphic record. *J. Geol.* **95** (1), 1–14.

Berner, E.K., Berner, R.A., 1987. *The Global Water Cycle: Geochemistry and Environment*. Prentice-Hall, Inc, Englewood Cliffs, NJ, p. 397.

Boone, R.D., Nadelhoffer, K.J., Canary, J.D., Kaye, J.P., 1998. Roots exert a strong influence on the temperature sensitivity of soil respiration. *Nature* **369**, 570–572.

Brook, F.Z., *A Late-Quaternary Pollen Record from the Middle Ogeechee River Valley, southeastern Coastal Plain*, Georgia, M.A. Thesis, University of Georgia, Athens, GA, 1996.

Brook, G.A., Folkoff, M.F., Box, E.O., 1983. A world model of soil carbon dioxide. *Earth Surf. Processes Landforms* **8**, 79–88.

Bruce, R.R., Dane, J.H., Quisenberry, V.L., Powell, N.L., Thomas, A.W., 1983. Physical characteristics of soil in the southern region: Cecil. *South. Cooper. Ser. Bull.* **267**, 185.

Cerling, T.E., 1984. The stable isotopic composition of modern soil carbonate and its relationship to climate. *Earth Planet. Sci. Lett.* **71**, 229–240.

Craig, H., 1954. The geochemistry of the stable carbon isotopes. *Geochim. Cosmochim. Acta* **3**, 53–92.

Craig, H., 1957. Isotopic standards for carbon and oxygen and correction factors for mass spectrometric analysis. *Geochim. Cosmochim. Acta* **12**, 133–144.

Huntington, T.G., 1995. Carbon sequestration in an aggrading forest ecosystem in the southeastern USA. *Soil Sci. Soc. Am. J.* **59** (5), 1459–1467.

Jackson, S.T., Whitehead, D.R., 1993. Pollen and macrofossils from Wisconsinan interstadial sediments in northeastern Georgia. *Quater. Res.* **39**, 99–106.

Jensen, L.S., Mueller, T., Tate, K.R., Ross, D.J., Magid, J., Nielsen, N.E., 1996. Soil surface CO_2 flux as an index of soil respiration in-situ -a comparison of 2 chamber methods. *Soil Biol. Biochem.* **28** (10-11), 1297–1306.

Lasaga, A.C., 1998. *Kinetic Theory in the Earth Sciences*. Princeton University Press, Princeton, New Jersey, p. 811.

Leigh, D.S., Feeney, T.P., 1995. Paleochannels indicating wet climate and lack of response to lower sea level, southeast Georgia. *Geology* **23** (8), 687–690.

Melear, N.D., 1998. *Crystal Properties of Goethite and Hematite from Three Weathering Profiles of the Georgia Piedmont*, Ph.D Thesis, University of Georgia, Athens.

Raich, J.W., Potter, C.S., 1995. Global patterns of carbon-dioxide emissions from soils. *Global Biogeochem. Cycles* **9** (1), 23–36.

Raich, J.W., Schlesinger, W.H., 1992. The global carbon dioxide flux in soil respiration and its relation to vegetation and climate. *Tellus* **44B**, 81–99.

Raner, K., *MacCurveFit v. 1.4—A Program to Fit User Defined Functions to a Set of Data Points*, Public domain software, 77 Therese Ave Mt Waverley, Vic 3149 Australia.

Schroeder, P.A., West, L., 2005. Weathering profiles developed on Granitic and Mafic terrains in the area of Elberton, Georgia. In: Roden, M., Schroeder, P.A., Swanson, S. (Eds.), *Geologic Investigations of Elberton Granite and Surrounding Rocks*, *Georgia Geological Society Guidebook*, Vol. 25. The Georgia Geological Society, Atlanta, GA, pp. 55–80.

Schroeder, P.A., Melear, N.D., 1999. Stable carbon isotopic signatures preserved in authigenic gibbsite from a forested granitic regolith: Panola Mt., Georgia, USA. *Geoderma* **91**, 261–279.

Schroeder, P.A., Melear, N.D., Bierman, P., Kashgarian, M., Caffee, M., 2001. Gibbsite growth ages for the regolith in the Georgia Piedmont. *Geochim. Cosmochim. Acta* **65** (3), 381–386.

Stuiver, M., Polach, H.A., 1977. Discussion; reporting of C-14 data. *Radiocarbon* **19** (3), 355–363.

White, A.F., 1995. Chemical weathering rates of silicate minerals in soils. In: White, A.F., Brantley, S.L. (Eds.), *Chemical Weathering Rates of Silicate Minerals*. Mineralogical Society of America, Blacksburg, VA, pp. 407–462.

Yapp, C.J., Poths, H., 1994. Productivity of pre-vascular continental biota inferred from the $Fe(CO_3)OH$ content of goethite. *Nature* **368**, 49–51.